# Microphase separated structure, surface composition and blood compatibility of segmented poly(urethaneureas) with various soft segment components

**Atsushi Takahara, Jun-ichi Tashita, Tisato Kajiyama and Motowo Takayanagi**
*Department of Applied Chemistry, Faculty of Engineering, Kyushu University, Hakozaki, Higashi-ku, Fukuoka 812, Japan*

**and William J. MacKnight**
*Polymer Science and Engineering Department, University of Massachusetts, Amherst, Massachusetts 01003, USA*
*(Received 3 November 1983; revised 16 January 1984)*

Properties, surface composition, and blood compatibility of segmented poly(urethaneureas) (SPUU's) with various soft segment components were investigated. The microphase separated structure between hard and soft segments improved with an increase in molecular weight ($\bar{M}_n$) of polyether diol in soft segment. The amount of absorbed water depended on the nature of the polyether component. X-ray photoelectron spectra of the surface of SPUU revealed that the surface composition depended on $\bar{M}_n$ and surface free energy of polyether component. Blood compatibility of SPUU depended on the state of microphase separated structure and surface composition.

**(Keywords: blood compatibility; microphase separation; soft segment; X-ray photoelectron spectroscopy (XPS); segmented poly(urethaneurea))**

## INTRODUCTION

Segmented poly(urethaneurea) (SPUU) is a linear elastomer consisting of soft and hard segments. The hard segment contains the urea group which shows a strong hydrogen bonding character and aggregates into paracrystal-like domains. In the case of the ordinary SPUU of which the hard segment content is below 40%, the soft segment forms the continuous phase. The hard segment domains play a role as physical crosslinks or fillers and the soft segment corresponds to the network chain in ordinary rubber. The existence of the hard segment domain may give SPUU an excellent mechanical strength[1].

The excellent blood compatibility of SPUU was discovered by Boretos and Pierce[2,3]. They also noticed the excellent mechanical properties of SPUU and applied it to a blood pump for an artificial heart system. However, little attention has been paid to the relationship between the blood compatibility and the structure of SPUU. In 1972, Lyman and coworkers synthesized SPUU from 4,4'-diphenylmethane diisocyanate (MDI), poly(propylene glycol) (PPG), and ethylenediamine (EDA) (molar ratio of 2:1:1) and examined the effect of molecular weight of PPG on the blood compatibility[4], the absorption of plasma protein[5], and the cell growth characteristics[6]. Excellent blood compatibility was observed at a molecular weight of PPG of 1025. Lyman *et al.* suggested that the blood compatibility was closely related to the domain size of SPUU[4,7]. Similar phenomena have been observed for other block or graft copolymer systems[8-10]. In our previous reports, we suggested that the microphase domain size and the degree of microphase separation have a considerable influence upon the blood compatibility of SPUU[11,12].

In this study, four series of SPUU were synthesized from poly(ethylene glycol) (PEG), poly(propylene glycol) (PPG), poly(tetramethylene glycol) (PTMG), and polybutadiene (PBD) as the soft segments. The physical and structural characterizations were performed using differential scanning calorimetric (d.s.c.), dynamic viscoelastic, stress–strain, X-ray photoelectron spectroscopic (XPS), and water absorption measurements. The blood compatibility was evaluated by the interaction between blood platelets and SPUU.

## EXPERIMENTAL

### *Materials*

*Table 1* shows the chemical composition of the segmented poly(urethaneureas) (SPUU's) used in this experiment. SPUU's were synthesized by a two-stage modified solution polymerization method[13]. The polyether diols employed were poly(ethylene glycol) (PEG), poly(propylene glycol) (PPG), poly(tetramethylene glycol) (PTMG), and hydroxy terminated polybutadiene (PBD). The number average molecular weight ($\bar{M}_n$) of these polyethers varied from 200 to 4000. The functionality of PBD is 1.96. Infra-red analysis of PBD yielded a

0032-3861/85/070987-10$03.00

**Table 1** Chemical composition of segmented poly(urethaneureas)

| Sample | Hard segment | Soft segment | $\bar{M}_n$ of polyether diol | Solvent |
|---|---|---|---|---|
| PEG $\bar{M}_n$–E | MDI–EDA | MDI–PEG ($\bar{M}_n$) | 200, 400, 600, 1000, 2000 | DMF |
| PPG $\bar{M}_n$–E | MDI–EDA | MDI–PPG ($\bar{M}_n$) | 400, 700, 1000, 2000, 3000 | DMF |
| PTMG $\bar{M}_n$–E | MDI–EDA | MDI–PTMG ($\bar{M}_n$) | 1200, 1900, 2600, 4000 | DMF |
| PBD $\bar{M}_n$–E | MDI–EDA | MDI–PBD ($\bar{M}_n$) | 2120 | DMAc/THF |
| Biomer | MDI–EDA | MDI–PTMG ($\bar{M}_n$) | 1800 | DMAc |

Soft segment:

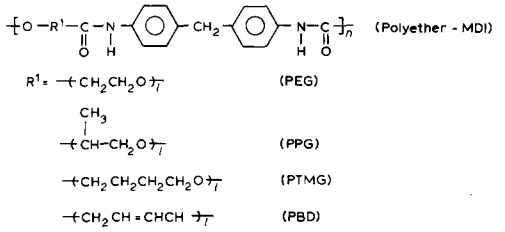


Hard segment:

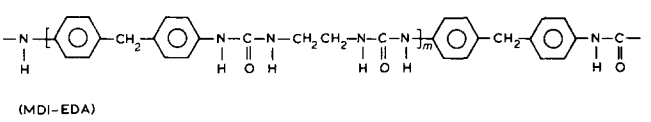

(MDI-EDA)

vinyl content of 55%, a *trans* content of 35%, and a *cis* content of 10%[14]. These polyether diols were dehydrated under vacuum at 373 K for 3 h. 4,4′-Diphenylmethane diisocyanate (MDI), dimethyl sulphoxide (DMSO), and dimethyl acetamide (DMAc) were distilled under reduced pressure. Ethylene diamine (EDA), methyl isobutyl ketone (MIBK), and tetrahydrofuran (THF) were distilled at atmospheric pressure. In the prepolymer reaction, the polyether diol was end-capped with MDI at 388 K for 90 min under a dried nitrogen purge. The molar ratio of MDI to polyether was 2:1. The following solvents were used for polymerization: a 1:1 mixture of DMSO and MIBK for PEG, PPG, and PTMG, and a 1:1 mixture of DMAc and THF for PBD. These prepolymers were cooled to room temperature and reacted with EDA for 60 min. The molar ratio of MDI to EDA was 2:1. The purification of SPUU was accomplished by precipitation from solution after polymerization. The precipitate was immersed in methanol for 15 h and washed with methanol. These SPUU's were dried *in vacuo* at 373 K for 10 h. The soft segment of SPUU consists of polyether diol and MDI. Each specimen has a different hydrophilicity of the polyether in the soft segment. The hard segment is composed of EDA and MDI. The molar composition is 2:1:1 in MDI:EDA:polyether diol. These specimens are designated 'X $\bar{M}_n$–E', where X represents various types of polyether diols with number average molecular weight of $\bar{M}_n$ and E represents ethylene diamine. For example, PTMG 1900–E represents a SPUU containing the soft segment composed of PTMG with $\bar{M}_n$ of 1900 and MDI, and the hard segment composed of MDI and EDA. Film specimens of PEG $\bar{M}_n$–E, PPG $\bar{M}_n$–E, and PTMG $\bar{M}_n$–E were cast on clean glass plates at 333 K from their dimethyl formamide (DMF) solutions. In the case of PBD 2120–E, the casting solvent employed was a 1:1 mixture of DMAc and THF. Solution grade Biomer, a commercially available SPUU for biomedical applications, was used as a reference specimen for blood compatibility. Films of Biomer were cast on clean glass plates at 338 K from a DMAc solution. These film specimens were washed with ethanol and dried *in vacuo*. The absence of residual solvent in these SPUU's was verified from the infra-red spectra of the film specimens.

*Physical and structural characterization*

*Water absorption test.* A disc plate of SPUU with a diameter of 4 mm and a thickness of 0.5 mm was die-cut from each film specimen. These disc plates were extensively dried *in vacuo* and were weighed with an ultra-precision balance. The discs were then soaked in deionized water at 310 K for 48 h and were weighed after removing water on the film surface with filter paper. The absorbed water content of each specimen was evaluated from the weight difference before and after soaking in water.

*Dynamic viscoelastic measurement.* The temperature dependences of dynamic viscoelastic storage and loss moduli were measured with a Rheovibron DDV-IIC (Toyo Baldwin Co., Ltd.) at 11 Hz under a dried nitrogen purge.

*Differential scanning calorimetry (d.s.c.).* D.s.c. thermograms from 150 to 400 K were obtained using a differential scanning calorimeter, UNIX (Rigaku Denki Co., Ltd.) at a heating rate of 10 K $min^{-1}$ under a dried nitrogen purge. The sample weight was $20 \pm 2$ mg.

*Stress–strain measurement.* Uniaxial stress–strain experiments were made with a Tensilon UTM III-500 (Toyo Baldwin Co., Ltd.) at 298 K at a cross head speed of 300 cm $min^{-1}$. Samples were die-cut from a sheet of SPUU film 0.4 mm in thickness. A specimen gauge length was about 15 mm long and 5 mm wide.

*X-ray photoelectron spectroscopy (XPS).* The XPS spectra were obtained on a Model 650B photoelectron spectrometer (du Pont Instrument Co., Ltd.) employing a magnesium anode ($MgK\alpha = 1253.6$ eV) which was operated at 7 kV and 36 mA. Samples were generally mounted with double stick tape. The charging shift was referred to the $C_{1s}$ line emitted from the saturated hydrocarbon at 285.0 eV. There was no visible damage to the sample surface during the exposure time involved in these measurements.

*Evaluation of blood compatibility of SPUU's*

Blood compatibility of SPUU's was evaluated by the degree of interaction between blood platelets and the film surface of SPUU. Film specimens of SPUU were soaked in platelet rich plasma (PRP) freshly prepared from a normal healthy adult and stored at 310 K in siliconized petri dishes on a laboratory shaker. After storage of 60 min, the films were rinsed with phosphate buffer

solution (PBS: Ionic strength, $I=0.2$, pH = 7.4) under gentle agitation to remove weakly adhered platelets. The adhered platelets on the film surface of SPUU were fixed with 1.5% glutaraldehyde in PBS for 15 h at 277 K and dehydrated with acetone graded series. These films were coated with Au–Pd, and the morphology of the adhered platelets was observed with a scanning electron microscope S-430 (Hitachi Co., Ltd.).

## RESULTS AND DISCUSSION

### *Physical and structural characterizations of SPUU*

*Water absorption of SPUU.* Water absorption tests were carried out in order to clarify the effect of the $\bar{M}_n$ of the polyether diol on the hydrophilicity of SPUU. *Figure 1* shows the variation of water content in SPUU with $M_n$ of polyether in the soft segment. The specimens were immersed in deionized water for 48 h at 310 K. The water content of SPUU increased with an increase in surface free energy of the polyether component. PEG 2000–E showed a large water absorption, characteristic of a hydrogel. On the other hand, PBD 2120–E showed fairly low water absorption due to the hydrophobic character of the PBD segment. In the cases of PPG $\bar{M}_n$–E and PTMG $\bar{M}_n$–E, the absorbed water content gradually increased with a decrease in $\bar{M}_n$ of the polyether. This increase in absorbed water content is ascribed to a relative increase in weight fraction of the hard segment for which the surface free energy is larger than those of PPG and PTMG. However, since the hard segments form paracrystalline domains, the real contribution of the hard segment to the hydrophilic property may be reduced below that expected from the surface tension calculated by means of the parachor[15].

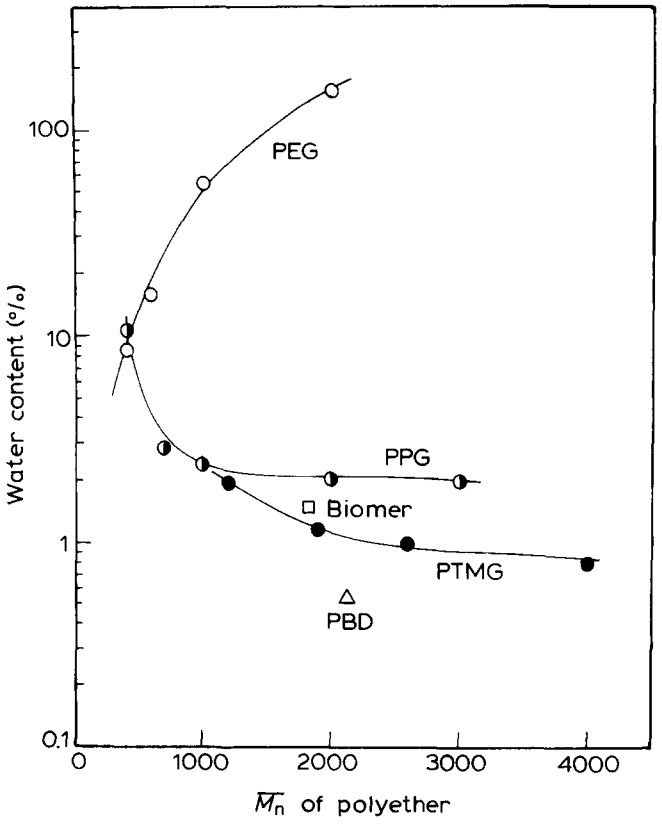


**Figure 1** Variation of water content of PEG $\bar{M}_n$–E, PPG $\bar{M}_n$–E, PTMG $\bar{M}_n$–E, PBD 2120–E and Biomer with $\bar{M}_n$ of polyether after immersing in deionized water for 48 h at 310 K

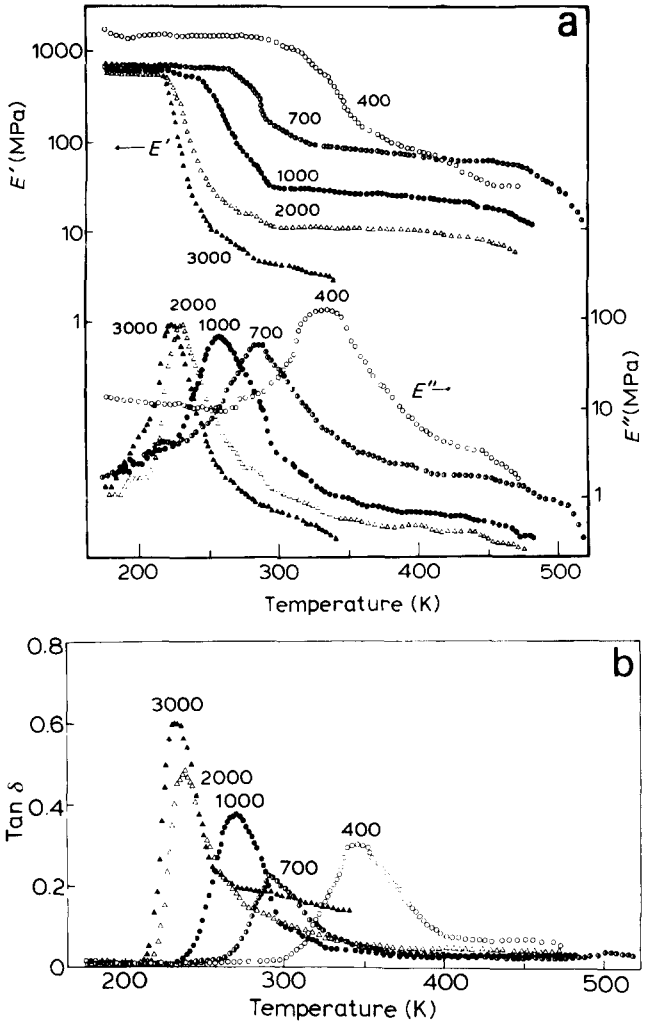


**Figure 2** Temperature dependences of $E'$, $E''$, (a) and tan $\delta$ (b) for PPG $\bar{M}_n$–E at 11 Hz

The absorbed water content of PEG $\bar{M}_n$–E increased with an increase in $\bar{M}_n$ of PEG. This finding indicates that the PEG segment becomes apparently more hydrophilic than the hard segment sequence. Consequently, the soft segment in PEG $\bar{M}_n$–E may show a larger surface free energy than that of the hard segment. These results suggest that the surface free energy gap between the hard and soft segment domains in PEG $\bar{M}_n$–E is opposite to those in PPG $\bar{M}_n$–E and PTMG $\bar{M}_n$–EDA.

*Temperature dependences of dynamic viscoelasticity. Figure 2* shows the temperature dependences of $E'$, $E''$ (a) and tan $\delta$ (b) for PPG $\bar{M}_n$–EDA. These SPUU's exhibit a single major absorption peak labelled the $\alpha_a$-peak. The $\alpha_a$-absorption shifts to higher temperatures and its $E''$ or tan $\delta$ peak width becomes broader with a decrease in $\bar{M}_n$ of PPG. As the number of polyether units in the prepolymer sequence is greater than *ca.* 3, even in case of $\bar{M}_n = 400$, the soft segment consisting of PPG and MDI is long enough to exhibit micro-Brownian motion. On the basis of the long period of SPUU measured by small-angle X-ray scattering, the numbers of polyether units in the soft segment are around 5[11]. This $\alpha_a$-absorption is associated with the glass transition temperature of the soft segment. The dependences of the $\alpha_a$-peak temperature and the peak width for the $\alpha_a$-absorption on $\bar{M}_n$ of PPG indicate that the microphase separation between the hard and soft segments becomes more distinct and the mole-

cular environment in each phase becomes more uniform with an increase in $\bar{M}_n$ of PPG. Since the weight fraction of the hard segment in PPG 400–E is 59%, the hard segment may form a continuous phase in which it mixes with the soft segment to a considerable extent. A fair decrease in $E'$ at around 450 K may be attributed to dissociation of hydrogen bonding or melting of the hard segment domains[11]. The decrease in $E'$ for PPG 400–E is observed at lower temperatures (~400 K) than in the case for other PPG $\bar{M}_n$–Es. This result also indicates that the hard segment in PPG 400–E is thermally less stable than in other PPG $\bar{M}_n$–E's due to phase mixing between the hard and soft segments.

*Figure 3* indicates the temperature dependences of $E'$, $E''$, (a) and $\tan\delta$ (b) for PTMG $\bar{M}_n$–E. The $\alpha_a$- and $\gamma$-absorptions are observed at around 210 and 150 K, respectively. the $\gamma$-absorption was assigned to a local mode motion of methylene sequences of PTMG. The $\alpha_a$-absorption arises from micro-Brownian segmental motion of amorphous PTMG associated with the glass transition[16]. The $\alpha_a$-absorption peak temperature of PTMG $\bar{M}_n$–E shifts to lower temperatures with an increase in $\bar{M}_n$ of PTMG. It seems reasonable to consider that the $\alpha_a$-absorption temperature increases with an increase in degree of phase mixing between the hard and soft segments, since thermal molecular motion within the soft segment is more restricted by phase mixing with the hard segment. This indicates that the micro-Brownian segmental motion of PTMG in PTMG 1200–E is impeded due to the partial solubilization of hard segments in the soft segment phase. The $\bar{M}_n$ dependence of the $\alpha_a$-absorption peak temperature for PTMG $\bar{M}_n$–E is small above $\bar{M}_n = 1900$, but the peak magnitude for the $\alpha_a$-relaxation process decreased with an increase in $\bar{M}_n$ of PTMG. Also, an additional relaxation process is observed as a shoulder of the $\alpha_a$-absorption peak in the case of $\bar{M}_n$ above 1900. This absorption process is assigned to a melting process of the crystalline phase of PTMG, being labelled as the $\alpha_f$-absorption process[16]. The $\alpha_f$-absorption peak for PTMG 1200–E is not clearly observed due to a low fraction of crystalline PTMG phase as shown by d.s.c. result of *Figure 5*. In the cases of PTMG 2600–E and PTMG 4000–E, the $\alpha_f$-absorption peak shifts to higher temperatures and is observed as a well separated peak. These $\alpha_a$- and $\alpha_f$-relaxation behaviours may indicate that the degree of phase separation between the hard and soft segments became distinct with an increase in $\bar{M}_n$ of PTMG. In the case of Biomer, similar dynamic viscoelastic behaviour to that of PTMG 1900–E was observed except for the small absorption peak at 300 K which has not been assigned to any molecular motion[11,17].

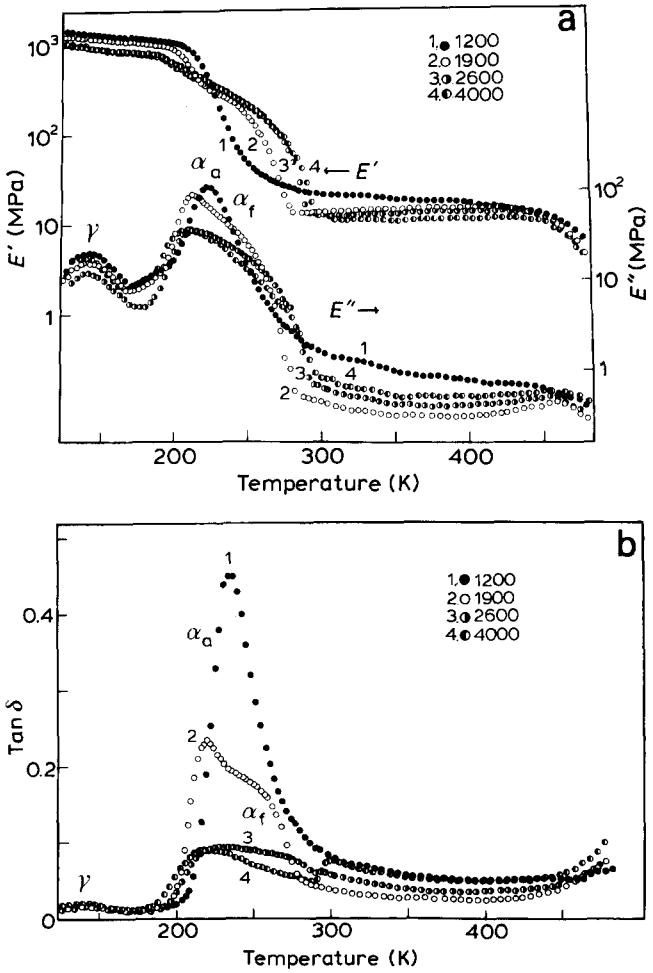


**Figure 3** Temperature dependences of $E'$, $E''$, (a) and $\tan\delta$ (b) for PTMG $\bar{M}_n$–E at 11 Hz

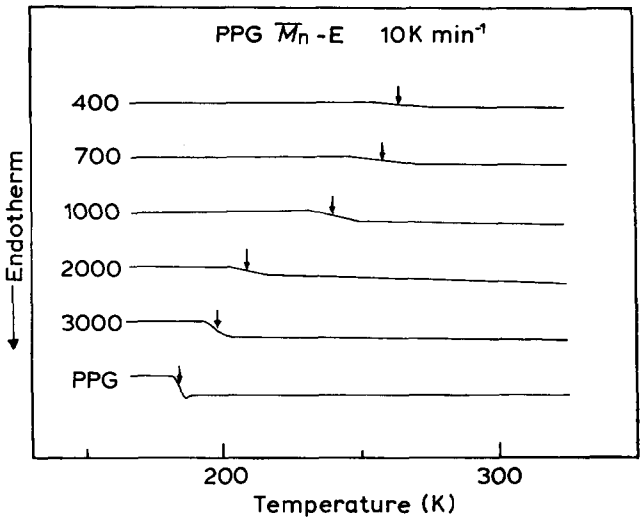


**Figure 4** D.s.c. thermograms for PPG $\bar{M}_n$–E and PPG homopolymer ($\bar{M}_n = 3000$)

*Differential scanning calorimetry* (*d.s.c.*). Thermal transitions of SPUU's were measured by means of d.s.c. *Figure 4* shows the d.s.c. thermograms for PPG $\bar{M}_n$–E. An increase in specific heat corresponding to the glass transition of the soft segment was observed between 192 and 275 K, depending on the magnitude of $\bar{M}_n$. The glass transition temperature of the soft segment shifts to higher temperatures with a decrease in the $\bar{M}_n$ of PPG. These results indicate that a certain degree of phase mixing of the hard and soft segments occurs with a decrease in $\bar{M}_n$ of PPG. Also, the glass transition zone width increases with a decrease in $\bar{M}_n$ of PPG. This result suggests a wide heterogeneity in the molecular environment of PPG in PPG $\bar{M}_n$–E.

*Figure 5* illustrates the d.s.c. thermograms for PTMG $\bar{M}_n$–E. In the case of PTMG homopolymer with $\bar{M}_n$ of 4000, a sharp endothermic peak due to melting of the PTMG crystals is observed at 307 K but the glass transition behaviour is obscured due to the high crystallinity. A broad exotherm observed at around 250 K may be due to the crystallization of amorphous PTMG[18]. The melting point of PTMG in PTMG $\bar{M}_n$–E shifts to a lower

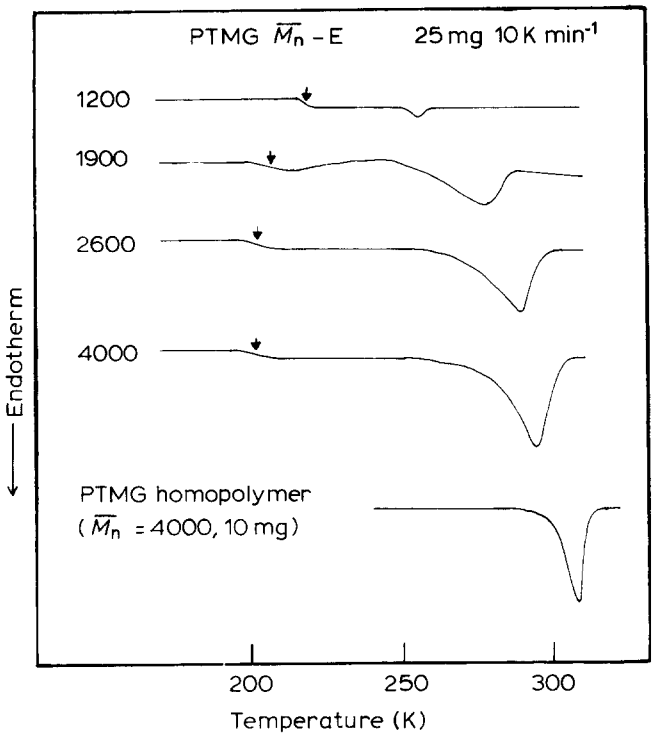


**Figure 5** D.s.c. thermograms for PTMG $\bar{M}_n$–E and PTMG homopolymer ($\bar{M}_n$ = 4000)

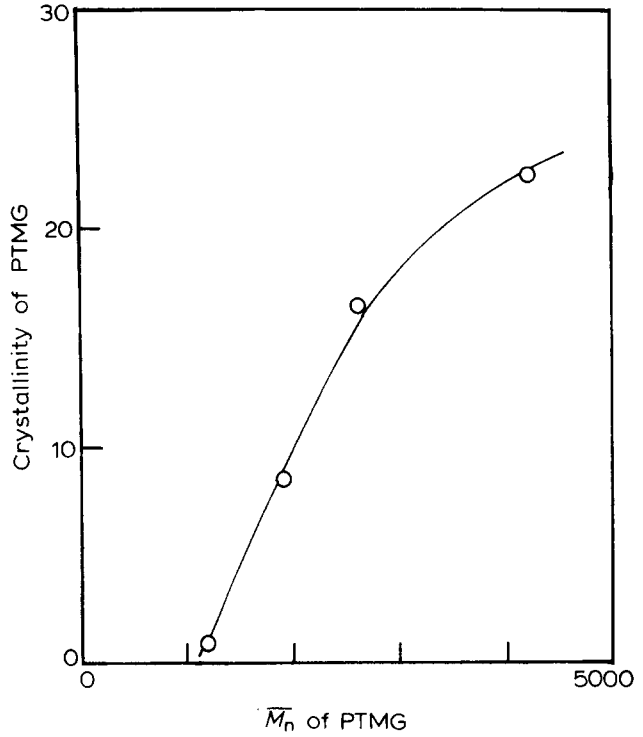


**Figure 6** Relationship between crystallinity of PTMG in PTMG $\bar{M}_n$–E and $\bar{M}_n$ of PTMG

temperature with decreasing $\bar{M}_n$ of PTMG. This depression of the melting point is attributed to a decrease in the size of the crystallites or an increase of incomplete crystalline phase due to phase mixing between the hard and soft segments. Since the glass transition temperature depends only slightly on $\bar{M}_n$ of PTMG, it is convenient to discuss the degree of phase separation on the basis of the degree of crystallinity of PTMG in the case of PTMG $\bar{M}_n$–E. *Figure 6* shows a plot of the crystallinity of PTMG in PTMG $\bar{M}_n$–E against $\bar{M}_n$ of PTMG. The degree of crystallinity of PTMG is determined from the ratio of the heat of fusion for PTMG $\bar{M}_n$–E to that of PTMG crystal[15]. The standard materials used to calculate enthalpy were indium (In), tin (Sn), and lead (Pb). The degree of crystallinity of PTMG increased with an increase in $\bar{M}_n$ of PTMG. This trend represents the fact that the crystallization of PTMG is more impeded by an increasing phase mixing for PTMG $\bar{M}_n$–E with smaller $\bar{M}_n$ of PTMG. The phase mixing may be caused by hydrogen bonding interactions between the soft segment ether oxygen and the urethane or urea N–H of phase mixed hard segment. A similar tendency on the crystallization of PEG in PEG $\bar{M}_n$–E was observed.

*Figure 7* shows the variation of glass transition temperature ($T_g$) and melting point ($T_m$) of polyether in the soft segment with $\bar{M}_n$ of polyether in polyether $\bar{M}_n$–E. The melting point of polyether is observed in the case of PTMG $\bar{M}_n$–E and PEG $\bar{M}_n$–E of which $\bar{M}_n$ of the polyether is larger than 1000. In all cases, the glass transition temperature decreases and the melting point increases with an increase in $\bar{M}_n$ of polyether. It is apparent from these results that the microphase separated structure of SPUU becomes more distinct with an increase in $\bar{M}_n$ of polyether in the soft segment. These phenomena are consistent with theoretical predictions regarding the microphase separation in multiblock copolymers[19].

*Stress–strain behaviour. Figure 8* shows the stress–strain curves of PPG $\bar{M}_n$–E at 298 K. The maximum of tensile strength was observed in the case of PPG 700–E. PPG 1000–E showed the maximum ultimate elongation value. Plastic yield is observed only for PPG 400–E of which the hard segment content is 59%. In the case of PPG 700–E, a rubber like behaviour is observed. These stress–strain results indicate that the continuous phase varies from the hard segment to the soft segment at a $\bar{M}_n$ of around 600. The true strength showed maximum at PPG 1000–E. The tensile strength and ultimate elongation for PPG 2000–E and PPG 3000–E are much smaller than those for PPG 1000–E. This result means that the hard segment does not act as an effective crosslinker or a filler when $\bar{M}_n$ of PPG is above 2000. The results of tensile tests for PEG $\bar{M}_n$–E and PTMG $\bar{M}_n$–E are summarized in *Table 2*.

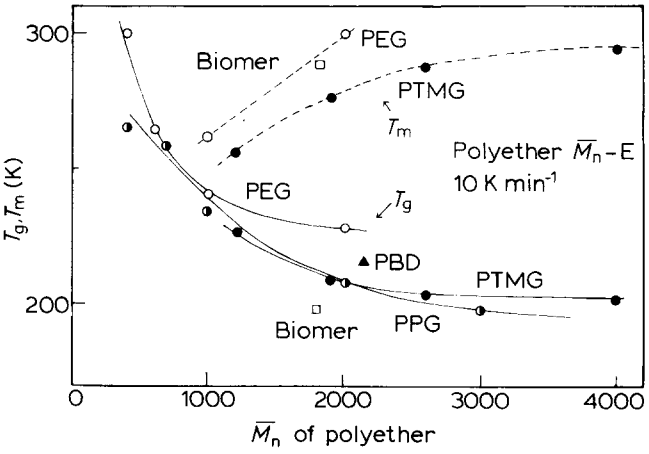


**Figure 7** Variation of glass transition temperature, $T_g$ and melting temperature, $T_m$ of soft segment (polymer) for polyether $\bar{M}_n$–E with $\bar{M}_n$ of polyether

*X-ray photoelectron spectroscopy (XPS).* *Figure 9* shows the X-ray photoelectron spectra (XPS) for $C_{1s}$, $N_{1s}$, and $O_{1s}$ for the air facing surface (AFS) and the substrate facing surface (SFS) of PPG 1000–E solution-cast on a clean glass plate. All spectra show three carbon peaks, one nitrogen peak, and one oxygen peak. The $C_{1s}$ peak corresponding to the aliphatic and aromatic carbon was observed at 285.0 eV. The $C_{1s}$ peak for ethereal carbon occurs at 286.3 eV. The $C_{1s}$ peak corresponding to the carbonyl carbon of urethane and urea groups was observed as a shoulder at 288.8 eV. The $N_{1s}$ peak occurs at 400.3 eV, corresponding to the nitrogen of urea and urethane groups. The $O_{1s}$ peak appears at 532.9 eV, corresponding to the oxygen of the polyether, and urethane and urea carbonyl. The intensity of $C_{1s}$ peak from the ethereal carbon is larger in AFS than that in SFS. Also, the ratio of the intensity of the $O_{1s}$ to $N_{1s}$ peaks on AFS is larger than that on SFS. Elemental analysis of these SPUU's revealed that the number ratio of oxygen to nitrogen atoms increased with an increase in $\bar{M}_n$ of the polyether. These results indicate that the PPG component was more abundant on AFS than on SFS due to the lower surface free energy of PPG compared with the hard segment component.

The signal intensity observed for a given core level can be described by the equation[20]

$$I_i = F_i N_i k_i \alpha_i \lambda_i \quad (1)$$

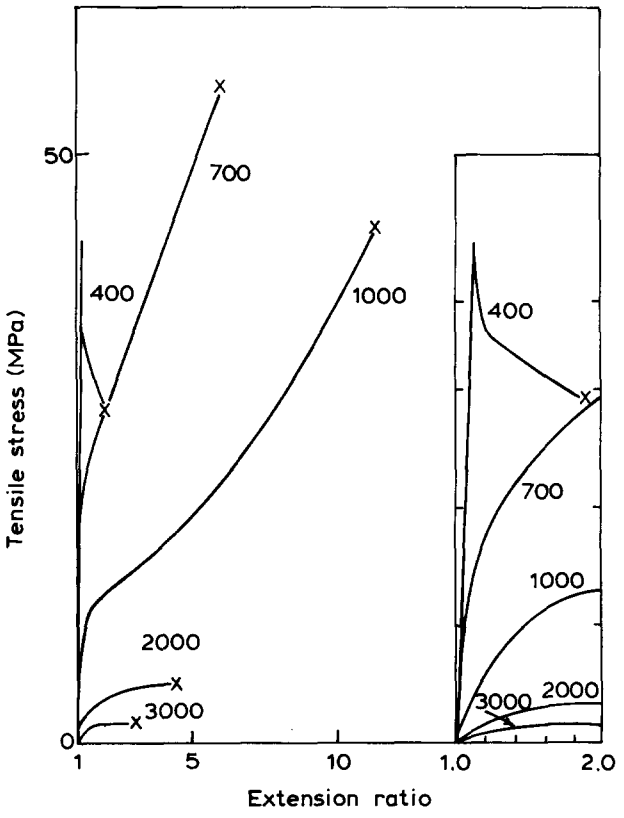


**Figure 8** Stress–strain curves for PPG $\bar{M}_n$–E at 298 K. Initial gauge length is 15 mm and extension rate is 300 mm $min^{-1}$

**Table 2** Tensile properties of segmented poly(urethaneureas)

| Sample | Initial modulus (MPa) | Ultimate strength (MPa) | Elongation at break (%) |
|---|---|---|---|
| PEG 400–EDA | 587 | 44.6* | 220 |
| PEG 600–EDA | 69.9 | 10.5* | 107 |
| PEG 1000–EDA | 17.5 | 32.8 | 1480 |
| PEG 2000–EDA | 7.4 | 13.4 | 1330 |
| PPG 400–EDA | 460 | 42.1* | 87 |
| PPG 700–EDA | 71.4 | 55.7 | 710 |
| PPG 1000–EDA | 41.1 | 43.8 | 1030 |
| PPG 2000–EDA | 12.9 | 4.9 | 350 |
| PPG 3000–EDA | 3.9 | 1.7 | 200 |
| PTMG 1200–EDA | 19.4 | 31.2 | 973 |
| PTMG 1900–EDA | 9.8 | 66.9 | 1530 |
| PTMG 2600–EDA | 9.6 | 55.2 | 1200 |
| PTMG 4000–EDA | 9.4 | 41.7 | 1820 |
| Biomer | 10.9 | 45.8 | 1560 |

*yield stress

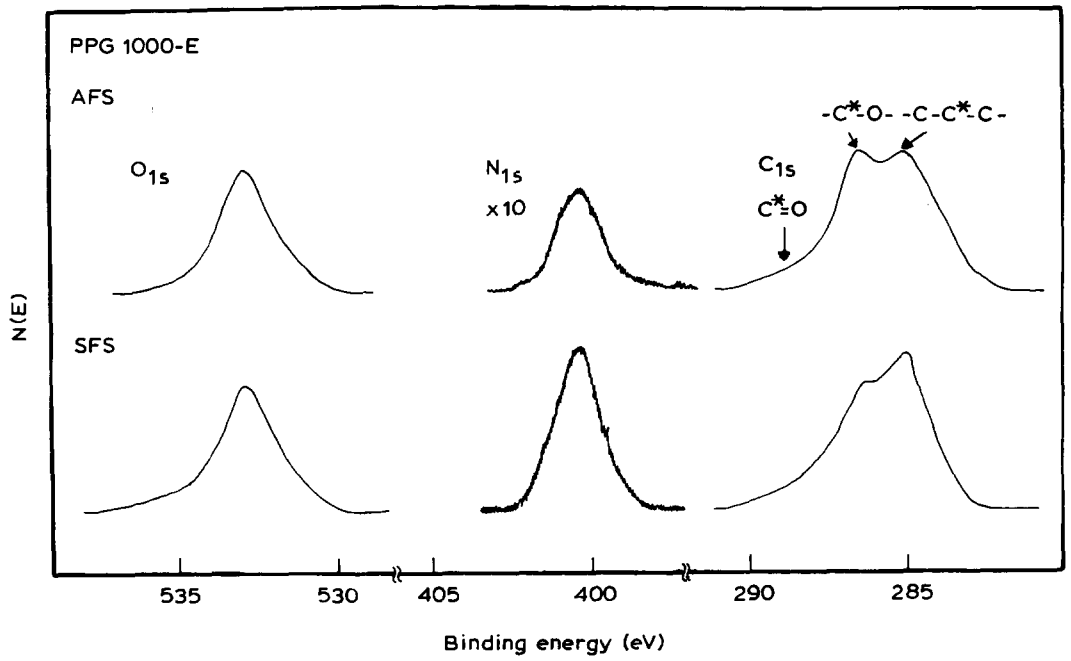


**Figure 9** X-ray photoelectron spectra for PPG 1000–E. AFS: air facing surface, SFS: substrate facing surface

where $F_i$ is the X-ray flux, $\alpha_i$ the cross-section for photoionization in the direction of the analyser, $N_i$ the number of the $i$ atoms in a given volume element, $k_i$ a spectrometer factor, and $\lambda_i$ the electron mean free path which depends on the kinetic energy of the photoelectron as well as the material through which it passes. The ratio of the number of atoms A to B in a volume element is given by

$$\frac{N_B}{N_A}=\frac{I_B \cdot F_A \cdot k_A \cdot \alpha_A \cdot \lambda_A}{I_A \cdot F_B \cdot k_B \cdot \alpha_B \cdot \lambda_B} \quad (2)$$

A rearrangement of equation (2) gives

$$\frac{N_B}{N_A}=\frac{I_B \cdot R_B}{I_A \cdot R_A} \quad (3)$$

where

$$R_i = 1/(F_i k_i \alpha_i \lambda_i)$$

$R$ is taken to be unity for $C_{1s}$ since one of the $R$ is an arbitrary parameter. The $R$ values used in this study were reported by Williams and Davis: 1.00 for $C_{1s}$, 0.344 for $O_{1s}$, and 0.524 for $N_{1s}$.

*Figure 10* shows the variation of the number ratio of oxygen to nitrogen atoms, O/N for PPG $\bar{M}_n$–E with $\bar{M}_n$ of PPG. The broken line means the magnitude of O/N evaluated from elemental analysis. As the number of oxygens in the soft segment is much larger than that of the carbonyl oxygens in the urethane or urea groups, it is reasonable to consider that O/N represents a relative soft segment concentration. O/N increases with an increase in $\bar{M}_n$ of PPG due to an increase in weight fraction of a soft segment component. In all cases, O/N on the AFS is larger than on SFS, indicating the abundance of PPG on AFS. This anisotropic segment distribution is due to the difference in surface free energy of the hard and soft segments. In the solvent-evaporating process, a thermodynamically stable surface state is attained, that is, the lower surface free energy component prefers to interface with air. A similar result was observed for PTMG $\bar{M}_n$–E. *Figure 11* represents the variation of O/N for PEG $\bar{M}_n$–E with $\bar{M}_n$ of PEG. In cases of PEG 1000–E and PEG 2000–E, O/N on AFS is smaller than that on SFS in contrast with the case of PTMG $\bar{M}_n$–E and PPG $\bar{M}_n$–E. Such an anisotropic distribution of the hard and soft segments is attributed to the lower surface free energy of the hard segment components in comparison with that of PEG. Disappearance of the anisotropic distribution of the hard and soft segment components on AFS and SFS in case of $\bar{M}_n = 400$ and 600 may reflect the phase mixing of the hard and soft segments.

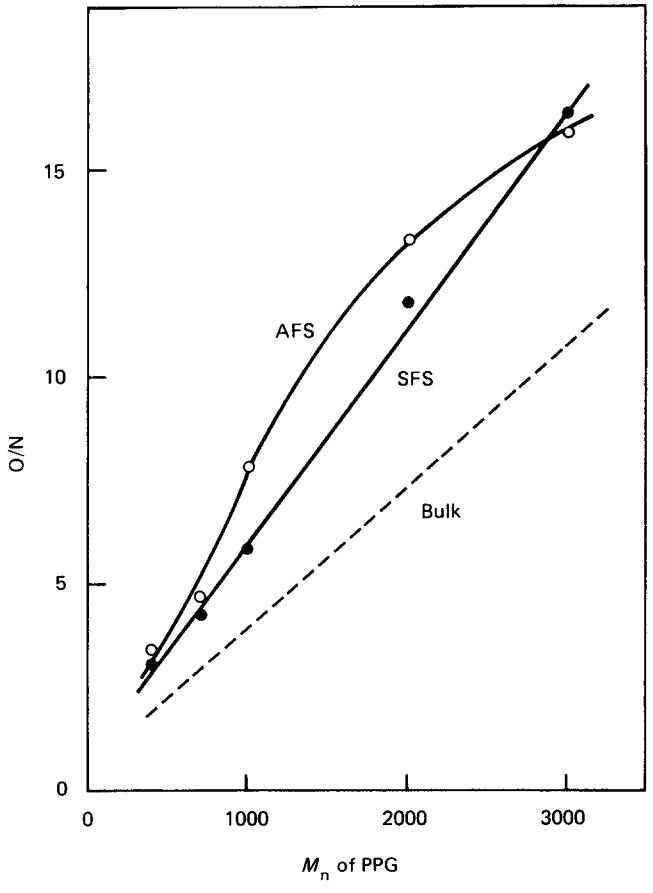


**Figure 10** Variation of the ratio of the number of oxygen to nitrogen atoms, O/N on AFS and SFS of PPG $\bar{M}_n$–E with $\bar{M}_n$ of PPG. The broken line means the magnitude of O/N evaluated from elemental analysis

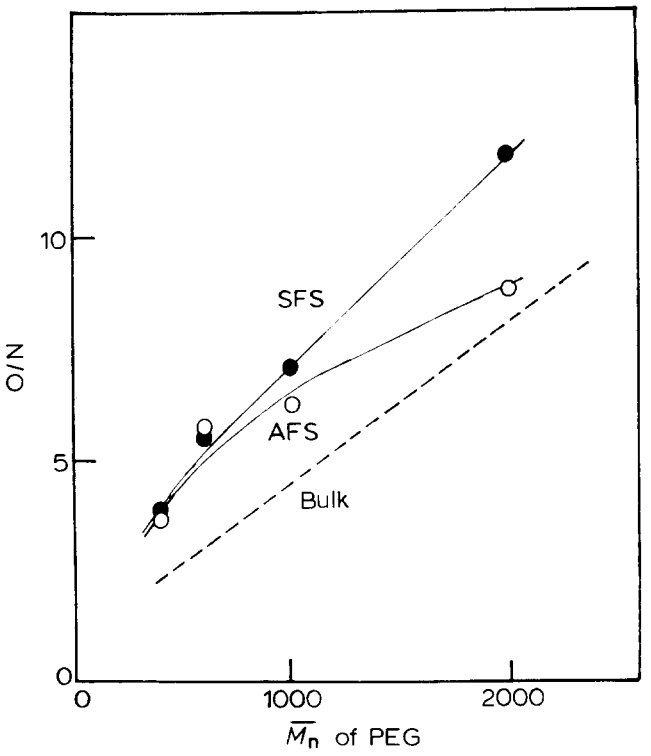


**Figure 11** Variation of the ratio of the number of oxygen to nitrogen atoms, O/N on AFS and SFS of PEG $\bar{M}_n$–E with $\bar{M}_n$ of PEG. The broken line means the magnitude of O/N evaluated from elemental analysis

*Blood compatibility*

Morphological changes of blood platelets on the polymer surface are closely related to the thrombogenicity of polymers. The blood compatibility of SPUU was evaluated from counting the number of adhered and deformed platelets on the film surface of SPUU. *Figure 12* shows the scanning electron photomicrographs of the typical morphology of the adhered and deformed platelets on the substrate surface. The morphology of adhered platelets was classified into three types based on the degree of deformation[11,22] as follows:

(I) attachment of platelets at a point of contact with substratum;

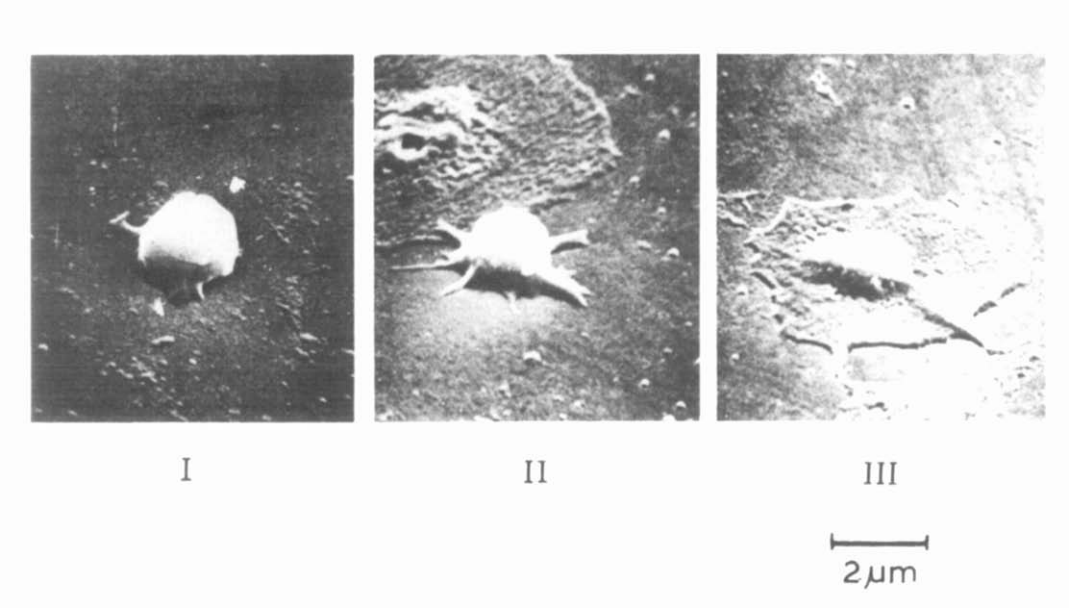


**Figure 12** Scanning electron photomicrographs of three types of adhered platelets on the surface of the substratum

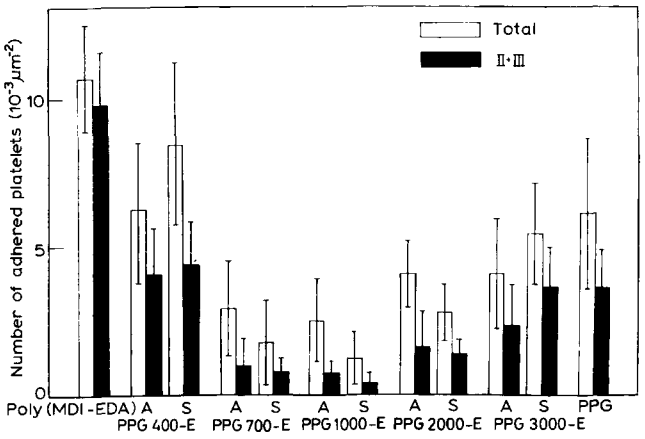


**Figure 13** Number of total adhered platelets and deformed platelets (types II and III) on AFS and SFS of PPG $\bar{M}_n$–A, homopolymer of hard segment (poly(MDI–EDA): polyurea), and poly(propylene glycol) after incubation in human platelet rich plasma for 60 min at 310 K

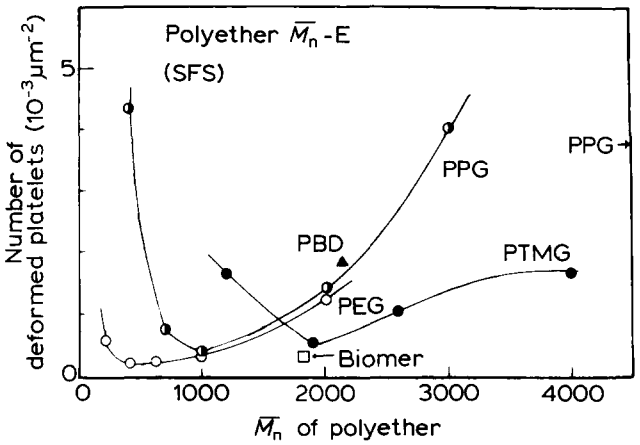


**Figure 14** Relationships between number of deformed platelets on SFS of PEG $\bar{M}_n$–E, PPG $\bar{M}_n$–E, PTMG $\bar{M}_n$–E, PBD 2120–E and Biomer and $\bar{M}_n$ of polyether after incubation in human platelets rich plasma for 60 min at 310 K

(II) centrifugal growth of filopodia;

(III) cytoplasmic webbing and flattening of the central mass.

The deformation of adhered platelets proceeds in the order of I, II and III with time and these morphological observations may be applied as a measure of blood compatibility. In the case of type I, the interaction between substrate and platelets is weak and adhered platelets can be easily removed from the film surface during rinsing with PBS. As the platelets of types II and III strongly adhere to the substrate, the number of adhered platelets of these types (number of deformed platelets) would be a measure of thrombogenicity.

*Figure 13* represents the number of total adhered platelets (types I, II and III) and deformed platelets (types II and III) on the surface of PPG $\bar{M}_n$–E, homopolymer of hard segment (polyurea) and poly(propylene glycol) after immersing in human platelets rich plasma (PRP) for 60 min at 310 K. The number of adhered and deformed platelets on the hard segment homopolymer and poly(propylene glycol) are larger than those of PPG $\bar{M}_n$–E showing microphase separated structure except for PPG 400–E. This finding indicates that the microphase separated structure of SPUU may be one of the factors controlling its blood compatibility. Blood compatibility of PPG 400–E is comparable to that of the hard segment homopolymer with respect to thrombogenicity. This poor blood compatibility of PPG 400–E may arise from its characteristic microphase separation in which the hard segment domain forms the continuous phase as shown in *Figure 8*. The best blood compatible surface is that of PPG 1000–E. As the degree of microphase separation of SPUU is improved with an increase in $\bar{M}_n$ of polyether[11], the blood compatibility of PPG $\bar{M}_n$–E may be closely related to these two structural factors.

*Figure 14* shows the variation of the number of deformed platelets on SFS of SPUU's with $\bar{M}_n$ of polyether. The numbers of deformed platelets on PEG $\bar{M}_n$–E, PPG $\bar{M}_n$–E and PTMG $\bar{M}_n$–E show minima at $\bar{M}_n$ of around 600, 1000 and 1900, respectively. On the basis of the number of deformed platelets, the blood compatibility of these SPUU's is comparable to that of Biomer. The $\bar{M}_n$ of polyether for the most blood compatible surface decreases with an increase in surface free energy of the

polyether component. This result indicates that the hydrophilic and hydrophobic balance of the SPUU surface has an important role in determining blood compatibility.

The concentration of the soft segment on the SPUU surface increases with an increase in $\bar{M}_n$ of PPG and PTMG because the magnitude of surface free energy increases in the order of PTMG, PPG, hard segment, and PEG as mentioned before. Therefore, the dependence of the number of deformed platelets on surface concentration of the polyether obtained with XPS must show a similar trend to that on $\bar{M}_n$ of polyether as shown in *Figure 14*, since the hydrophobic and hydrophilic balance on the SPUU surface is an important factor for blood compatibility. *Figure 15* shows the variation of the number of deformed platelets (types II and III) on film surface of SPUU with the ratio of oxygen to nitrogen atoms on its surface (O/N) which was evaluated by equation (3) on the basis of XPS measurement. The number of deformed platelets exhibits a minimum at around O/N = 5.5 for PEG $\bar{M}_n$–E, 6.0 for PPG $\bar{M}_n$–E, and 13.0 for PTMG $\bar{M}_n$–E. These results indicate that the concentration of soft segment on the film surface of SPUU influences the blood compatibility. The relationship between the number of deformed platelets and the ratio of the 286.3 eV (ethereal carbon) intensity to the 285.0 eV (aliphatic and aromatic carbon) intensity showed similar results to those of O/N. However, Sa da Costa and coworkers reported a positive correlation between the concentration of the ethereal carbon on the film surface of SPUU and the number of adhered platelets on SPUU[23]. This result is not consistent with our result mentioned above.

The mechanism of the blood compatibility of SPUU has been discussed by several authors[2-6,23-25]. Lyman and coworkers reported that the antithrombogenicity of PPG 1025–E was attributed to the selective absorption of albumin[4]. Matsuda and coworkers reported similar results on the blood compatibility of SPUU composed of PTMG ($\bar{M}_n$ = 2000), MDI and propylene diamine[24]. Some hydrogels which exhibited excellent blood compatibility did not adsorb any plasma protein[25]. The excellent blood compatibility of SPUU based on PEG has been interpreted by this mechanism[24]. However, our results revealed that PEG 2000–E is less blood compatible than PEG 1000–E and PEG 600–E. These different results indicate the need for further work to clarify the influences of chemical, physical and structural factors on blood compatibility of SPUU.

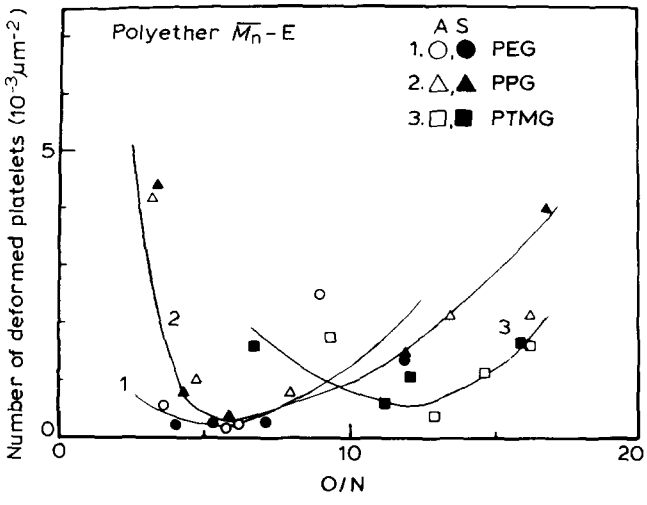


**Figure 15** Relationships between number of deformed platelets and surface concentration of soft segment (ratio of number of oxygen to nitrogen atoms) for PEG $\bar{M}_n$–E, PPG $\bar{M}_n$–E, and PTMG $\bar{M}_n$–E. Open symbols indicate AFS and closed ones, SFS

## CONCLUSIONS

D.s.c., dynamic viscoelastic, X-ray photoelectron spectroscopic (XPS), water absorption tests, and tensile testing were carried out in order to characterize the microphase separated structure of a series of segmented poly(urethaneureas) based on 4,4'-diphenylmethane diisocyanate, ethylene diamine, and polyethers with various surface free energies and molecular weights. Also, the blood compatibility of these SPUU's was evaluated by the degree of interaction between the blood platelets and the surface of SPUU films.

D.s.c. and dynamic viscoelastic measurements of these SPUU's revealed that the phase mixing between the hard and soft segments increased with a decrease in molecular weight of the polyether. The water absorption tests clarified the relative surface free energy of each segment. The magnitude of the surface free energy of the component decreases in the order of PEG, hard segment, PPG, PTMG and PBD. XPS spectra clarified the distribution of the hard and soft segments on the air and substrate facing surfaces. The anisotropic distribution of hard and soft segments on the surface of SPUU occurred due to the difference in surface free energy of each segment.

The blood compatibility of SPUU was better than that of the homopolymer of each hard or soft segment which constitutes SPUU. This means that microphase separated structures may affect blood compatibility of SPUU. The number of adhered and deformed platelets on SPUU's shows a minimum at a certain molecular weight of polyether ($\bar{M}_n$) or a certain surface concentration of soft segment (O/N), depending on the magnitude of surface free energy. This result indicates that the hydrophobic and hydrophilic balance of the SPUU film surface is one of the important factors determining blood compatibility.

## ACKNOWLEDGEMENTS

The authors wish to express their sincere thanks to Dr S. Inaba of the Department of Blood Transfusion, Kyushu University Hospital. We thank Mr N. Sakamoto and Prof. Y. Yamamoto of the Department of Mechanical Engineering, Faculty of Engineering, Kyushu University, for their generous advice, and assistance with XPS measurements.

## REFERENCES

1 Smith, T. L. *Polym. Eng. Sci.* 1977, **17**, 129
2 Boretos, J. W. and Pierce, W. S. *Science* 1967, **158**, 1941
3 Boretos, J. W. *Pure Appl. Chem.* 1980, **52**, 1851
4 Lyman, D. J., Knutson, K., McNeil, B. and Shibatani, K. *Trans. Am. Soc. Artif. Intern. Org.* 1975, **21**, 49
5 Lyman, D. J., Metcalf, L. C., Albo, Jr., D., Richards, K. F. and Lamb, J. *Trans. Am. Soc. Artif. Intern. Org.* 1974, **20**, 424
6 Lyman, D. J., Hill, D. W., Stirk, R. K., Adamson, C. and Mooney, B. R. *Trans. Am. Soc. Artif. Intern. Org.* 1972, **18**, 19
7 Shibatani, K., Lyman, D. J., Shieh, D. F. and Knutson, K. *J. Polym. Sci., Polym. Chem. Edn.* 1977, **15**, 1655
8 Imai, Y., Watanabe, A. and Masuhara, E. *Jpn. J. Artif. Org.* 1973, **2**, 95

9 Mori, Y., Nagaoka, S., Takiuchi, H., Kikuchi, T., Noguchi, N., Tanzawa, H. and Noishiki, Y. *Trans. Am. Soc. Artif. Intern. Org.* 1982, **28**, 459

10 Barenberg, S. A., Schultz, J. S., Anderson, J. M. and Geil, P. H. *Trans. Am. Soc. Artif. Intern. Org.* 1979, **25**, 159

11 Takahara, A., Tashita, J., Kajiyama, T. and Takayanagi, M. *Kobunshi Ronbunshu* 1982, **39**, 203

12 Takahara, A., Tashita, J., Kajiyama, T. and Takayanagi, M. *Rept. Progr. Polym. Phys. Jpn.* 1982, **25**, 841

13 Lyman, D. J. *Rev. Macromol. Chem.* 1966, **1**, 191

14 Brunette, C. M., Hsu, S. L., Rossman, M. MacKnight, W. J. and Schneider, N. S. *Polym. Eng. Sci.* 1981, **21**, 668

15 Van Krevelen, D. W. 'Properties of Polymers', 2nd Edn., Elsevier, Oxford, 1976, Ch. 8

16 Huh, D. S. and Cooper, S. L. *Polym. Eng. Sci.* 1971, **11**, 369

17 Lelah, M. D., Lambrecht, L. K., Young, B. R. and Cooper, S. L. *J. Biomed. Mater. Res.* 1983, **17**, 1

18 Henksketh, T. R., Van Bogart, J. W. C. and Cooper, S. L. *Polym. Eng. Sci.* 1980, **20**, 190

19 Krause, S. *Macromolecules* 1970, **3**, 84

20 Dilks, A. *Anal. Chem.* 1981, **53**, 802-A

21 Williams, D. E. and Davis, L. E. 'Characterization of Metal and Polymer Surfaces', Vol. 2 Polymer Surfaces, (Ed. L. H. Lee), Academic Press, New York, 1977, p. 53

22 Yonaha, C., Idezuki, Y., Hamaguchi, M., Watanabe, H., Mori, Y., Nagaoka, S., Kikuchi, T. and Tanzawa, H. *Jpn. J. Artif. Org.* 1980, **9**, 228

23 Sa da Costa, V., Brier-Russel, D., Trudell, III, G., Wauch, D. F., Salzmann, E. W. and Merril, E. W. *J. Colloid Interface Sci.* 1981, **76**, 594

24 Matsuda, T., Takano, H., Taenaka, Y., Toyosaki, T., Akutsu, T. and Nomura, S. *Polym. Prepr. Jpn.* 1982, **31**, 1793

25 Ikada, Y., Suzuki, M. and Tamada, T. *ACS Polym. Prepr.* 1983, **24(1)**, 19